2017 21st International Conference on Process Control (PC)
June 6–9, 2017, Štrbské Pleso, Slovakia

Studying the chemiresistor platform properties

Ladislav Fišer, Karel Kadlec, Jan Herbst
University of Chemistry and Technology
Department of Physics and Measurements
Technická 5, 166 28 Praha 6 - Dejvice, Czech Republic
Email: ladislav.fiser@vscht.cz

***Abstract*—In order to make a research of chemiresistors, having a suitable platform, on which studied layer can be created and measured is a necessity. Standard sensors are built upon ceramic base equipped with electrodes and heating or tempering elements. Here at Department of Physics and Measurements a transition to a KBI2 platform made by Tesla Blatná is being conducted. This particular model was chosen because at this time it is the only available one. Main purpose of this paper is mapping its properties, especially the homogeneity of temperature of the chip and overall its dynamic thermal properties. This platform was connected into the heating circuit and readouts of its internal temperature sensor (Pt_{1000}) were evaluated, the temperature was also observed using an thermal imager FLIR T 400 with a macro flyleaf. Calibration of thermal camera is also discussed as well, as determination of each area emissivity. The main result is description of temperature layout all over the chip of the platform and its step responses measured out of thermographical videos taken when the heating was switched on. These data can be further used as base for temperature regulation circuits design. Also quantification of uncertainties of the internal temperature sensor and temperature gradients, which cannot be neglected during sensor layer evaluation, is based upon these data. In the acquired data, symmetrical temperature layout by longitudinal axis is observed. Problems are seen in gradient over the chips length, for operating temperature 300 °C can this difference reach up to 100 °C.**

***Index Terms*—Chemiresistor, Temperature, Thermal imager, KBI2 platform**

1. Introduction

In order to study chemiresistors it is necessary to have some platform to prepare layer on. Standard chemiresistors are created upon ceramic base equipped with interdigital electrodes for contact with a sensor layer. This platform is further equipped with metal resistive heating element for its ability to reach desired temperature. This platform is usually built on a ceramic plate made of Al_2O_3 with platinum electrodes and heating element evaporated onto. Two configurations are possible for such platform - sensitive layer can be either on opposing sides of ceramic base or on the same side [1].

At Department of Physics and Measurements platforms of the first type were used up until now, but since they are not available anymore, a transition to the only available alternative had to be done. From now, Tesla KBI2 platform, which have both heating element and sensitive layer on the same side [2], will be used. Configuration of this platform is depicted on Figure 1.

The sensitive layer of chemirisistor consists of a semiconductor, thus it's resistivity depends on a temperature. Temperature fluctuation is one of the most disrupting factors [1]. The sensitivity for analyte also depends on a temperature. The operating temperature of many of layers is relatively close to destructive temperature, thus temperature gradients may have considerable impact on both stability and lifespan of a chemiresistor. Without the knowledge of thermal properties of a KBI 2 platform it is not possible to design a sensor properly or even determine the platform capabilities.

For our experiments this whole platform was soldered onto suitable connector (DIN 7), which served both as electrical connection and mechanical support. Next to it a thermal imager was also mounted. Electrical current for heating was supplied by Agilent E3631A controllable supply in range from 0 to 400 mA. The temperature sensor value was measured using Metex M3850D multimeter using measuring current of 50 μA (manufacturer of the platform allows currents up to 300 μA [2]). Main purpose of this experiments was to investigate whether there are any temperature gradients, and if so, to find them and also compare the integrated temperature sensor value with temperature measured by thermal imager. Because of thermal imagers ability to take video, dynamic properties of the platform were also investigated. Phase of heating platform up was captured, so the temperature step response was determined.

2. Thermography

Compact thermal imager FLIR T 400 [4], [5] was used for the thermographic measurement of the platform. The thermal camera is equipped with the microbolometric uncooled focal-plane array detector (FPA) with a resolution of 320 $\times$ 240 pixels. Parameters of the thermal imager: spectral range of 7.5 to 13 mm, 3 temperature ranges from -20 to 120 °C, from 0 to 350 °C and from 200 to

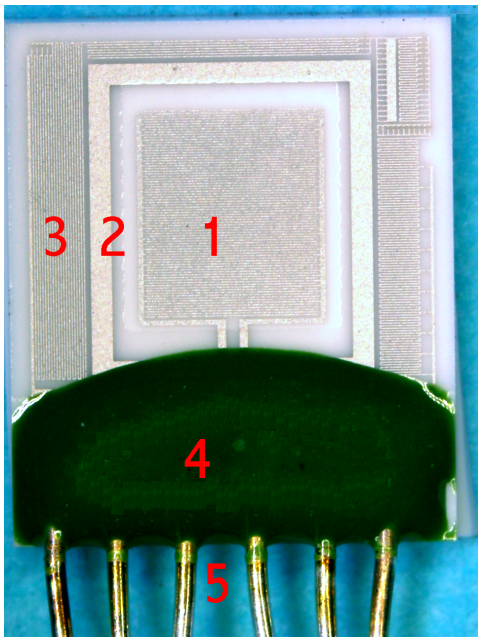

Figure 1. Sensor platform KBI2 macro photography, dimensions of ceramic base are 6.2×5.25 mm [2].
1 - interdigital electrode area
2 - 8 Ω resistive heating element
3 - Pt_{1000} temperature sensor area
4 - contact point ceramic cover
5 - 250μ m diameter Ag wire pins

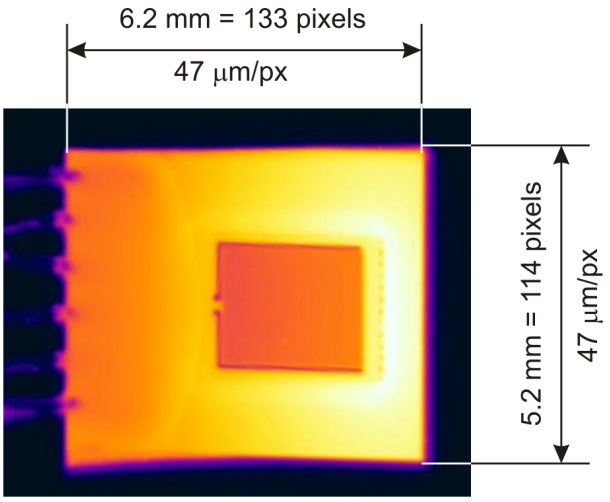

Figure 2. Thermogram resolution

TABLE 1. CALCULATED EMISSIVITIES FOR EACH AREA.

Area	Emissivity
Interdigital electrodes	0.47
Pt_{1000} temperature sensor	0.87
Heating element	0.87
Wire cover	0.91

1 200 °C, sensitivity 0.06 °C and accuracy ±2 °C. Macro lens 2 × (50 mm), which provides twice the increase in the size of the observed object can be used to measure small objects. In our case, the size of the object being measured was 6.2 mm × 5.2 mm and when using the macro lens, then this corresponds to 133 × 114 pixels on the thermogram (2). From the data thus follows that 1 pixel = 47 μm. Considering that the recognizable object should be of corresponding size 3 × 3 pixels, then from the above data show that on the thermogram can be recognize the details and analyze the temperature on the facets with a diameter of about 0.15 mm.

For calibration of the thermal imager was used blackbody Isotech Gemini (temperature range of 50 to 550 °C, temperature stability of ±0.1 °C, emissivity of cavity $\varepsilon = 0.995$ [6]. Thermal camera indications were compared at temperatures (155, 201, 250, 300, and 350) °C. Electronic circuits of the thermal imager calculate the temperature of the measured object according to the amount of radiant flux coming on to the detector. However, the radiation measured by the camera is not only dependent on the temperature of the object, but also on other parameters, in particular the emissivity of the measured object, the reflected radiation from surrounding objects and absorption of radiation through the atmosphere. For accurate temperature measurement is therefore necessary to compensate these interferences. The camera automatically compensates these interferences by specifying the appropriate parameters. Emissivity of the object is the most important parameter that must be properly determined. Emissivity of the object was determined that the platform was covered in paint with the defined emissivity ($\varepsilon = 0.96$). One half of the sensor was cover with paint of defined emissivity. Thermogram is depicted on Figure 3. It is obvious, that each areas has different emissivity. Covering one half of 5×6 mm platform in paint is not an easy task; on Figure 3 you can clearly see, that the boundary is not homogeneous. But the emissivity can still be obtained from this thermogram for areas further form the boundary. Using FLIR QuickReport software were then chosen points and areas in parts of platform symmetrically by the center of platform as symmetrical thermal distribution was assumed (later it was confirmed). By assuming the same actual temperature and comparing measured temperature, the emissivity was calculated for each area, TABLE 1, and later used for evaluation.

Another, smaller shapes can be also found on the surface of the platform, but their size is approximately at the threshold of the resolution of the thermal imager, so none of them were further considered. The fact, that the heating and temperature measuring area is covered with a thin layer of glass due to a sensor stability is making these measurements problematic. The interdigital electrodes area of course is not covered.

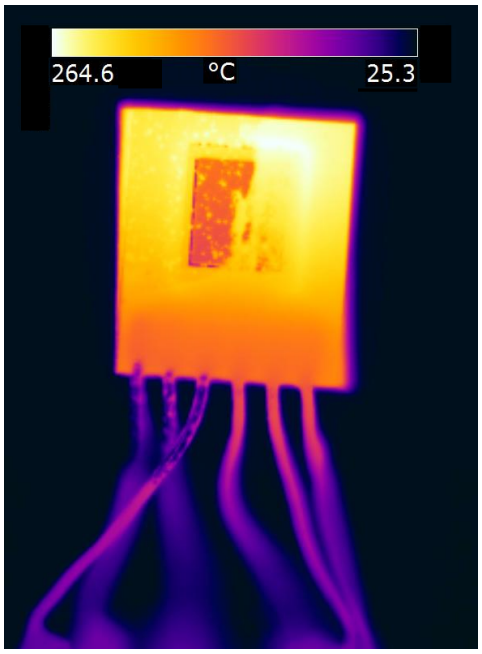

Figure 3. Thermogram of KBI2 platform, the right half is covered by paint $\varepsilon = 0.96$; emissivity of each area is determined by comparison of left and right halves.

3. Experimental results

Just by looking at Figures 4a, 4b it is clear, that temperature gradients are present. For their quantification FLIR QuickReport software was used to generate data and further chart of temperature along different cross-sections in dependency of position. At Figure 5 there is crosswise dependency. The independent parameter was horizontal position. It clearly evinced symmetrical behaviour, thus the middle point was marked as zero, range of this parameter is then -3 to +3, units are mm. At the Figure 6 the independent parameter is vertical position. Since this dependency in not symmetrical, the lowest point was chosen as zero making the range 0 to 6.3 mm.

Some points of the curves are missing, especially the points at the boundary between the heating element and the interdigtal electrodes. This absence is caused by clearly incorrect obtained value in the thermogram. The most presumable explanation is, that these parts did cause reflections thus emissivity could not be correctly determined for them. These points were excluded form the chart, they have no meaningful value as they would make the chart unclear. For global image of thermal distribution,they are not essential.

The chart at the Figure 5 demonstrates, that along the shorter edge (further called width) is almost constant, at the area of interdigital electrodes it remains in range from 266 to 270 °C with the minimum at the middle for the middle curve L3. Further it exhibits maximum at the area of heating element (about ± 1.5 mm at the X axis) at about 282 °C. The temperature sensor area (about ± 2.1 mm at the X axis)

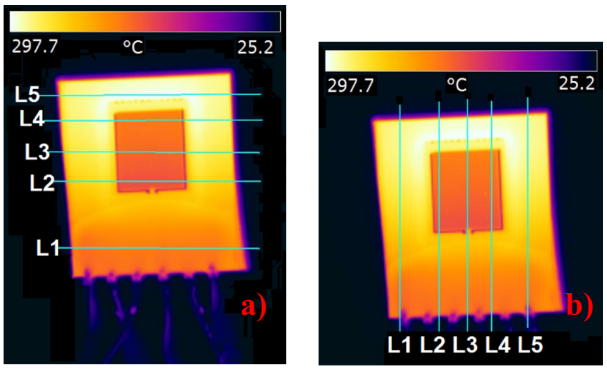

Figure 4. KBI2 thermogram, with emissivity correction (see TABLE 1)
a) Horizontal cross-sections are highlighted.
b) Vertical cross-sections are highlighted.
Temperature along these are data for charts on the Figures 5, 6.

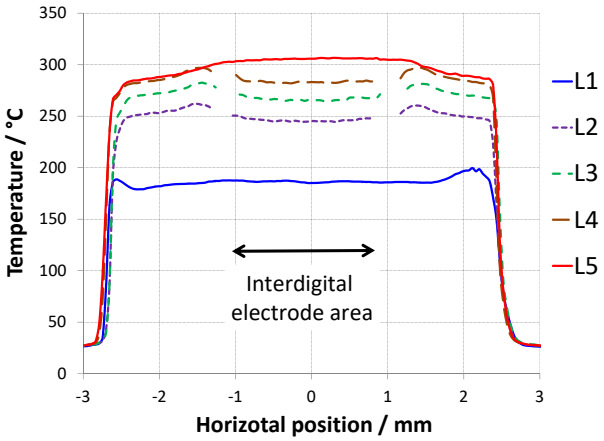

Figure 5. Graphical interpretation of temperature distribution at the KBI2 platform, horizontal position is the independent parameter, vertically is the platform divided into L1 to L5 curves
L1 - at the left border of the platform
L2 - at the left border of the interdigital electrodes area
L3 - the axis of the platform
L4 - at the right border of the interdigital electrodes area
L5 - at the right border of the platform

retains the similar temperature as the interdigital electrodes. It is favourable for the planned application of the platform.

The chart at the Figure 6 is less favourable. The vertical temperature gradient is rather large. The temperature is increasing with distance from pins. This is probably caused by both heat conduction of the pins and the absence of heating there (Figure 1). By considering only the area of interdigital electrodes, the temperature ranges from 250 to 290 °C making the difference substantial. The difference for the temperature sensor is even grater, its temperature reaches 300 °C.

For practical utilization the correspondence between the actual temperature in the area of the interdigital electrodes and the value of integrated temperature sensor is essential.

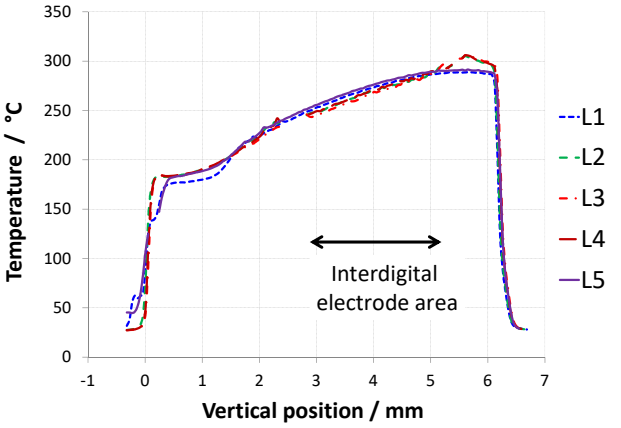

Figure 6. Graphical interpretation of temperature distribution at the KBI2 platform, vertical position is the independent parameter, horizontally is the platform divided into L1 to L5 curves
L1 - at the pins
L2 - at the bottom of the interdigital electrodes
L3 - at the middle of the interdigital electrodes
L4 - at the top of the interdigital electrodes
L5 - at the horizontal part of the heating element

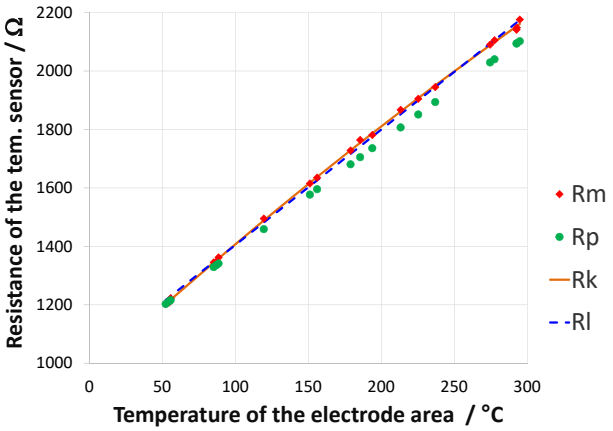

Figure 7. Comparison of temperature values.
Rm - measured resistance of integrated sensor
Rp - theoretical resistance of Pt_{1000}
Rk - theoretical value obtain using quadratic approximation
Rl - theoretical value obtain using linear approximation

This value is compared with the value from the thermal imager. Measured and calculated values can be seen in Figure 7. The X axis represents the mean value of the temperature of the interdigital electrode area. The Rm curve (resistance measured) depicts, which resistance was actually measured. Due to the Pt_{1000} type of sensor, the theoretical sensor resistance value, if the whole temperature sensor has the same temperature as the electrodes, can be calculated using (1). These values are in the curve Rp. Both this formula and these coefficients are taken form [3]

$$R_t = R_0 \cdot \left(1 + A \cdot t + B \cdot t^2\right) \tag{1}$$

The temperature value obtained by the thermal imager and the integrated sensor does not correspond well. This is not surprising, as the gradients are so high (Figure 5, 6). Therefore the coefficients were calculated for two relations between the temperature of electrodes and the resistance of integrated sensor. Firstly, the same formula, as for the Pt_{1000} sensor was assumed, but with different coefficients, secondly the sufficiency of simpler, linear relation (2) was tested.

$$R_t = R_0 \cdot \left(1 + A \cdot t\right) \tag{2}$$

The calculated resistance using the quadratic relation is labeled Rk, calculated resistance using linear relation is labeled Rl. Calculated values and correlation coefficients are in TABLE 2.

For the whole operating temperature range (from 50 to 350 °C) the temperature difference for values obtained using (1), (2) does not exceed 5 °C, while the gradient reaches 40 °C thus the linear relation (2) will be sufficient.

TABLE 2. CALCULATED COEFFICIENTS

Linear approximation			
R_0	1010	R^2	0.9986
A	$3.91 \cdot 10^{-3}$		
Quadratic approximation			
R_0	969	R^2	0.9996
A	$4.71 \cdot 10^{-3}$		
B	$-1.81 \cdot 10^{-6}$		

4. Dynamic properties of the platform

Our thermal imager was capable of taking a thermographical video thus research of dynamic properties of the platform was . The platform has been imaged, after start the heating current did a step of 400 mA. Subsequently this thermographical video was evaluated and temperature was obtained as a function of time. One of the measurements is depicted at Figure 8. In the fifth second the heating current has risen. The obtained data demonstrates, that this platform acts as system described by first order differential equation.

$$\tau \cdot \frac{dy}{dt} + y = k \cdot u \tag{3}$$

Ideal first order system (described by (3)) of course does not exist, and this system would be better describes by an equation of a higher order, in this particular case, first order approximation is sufficient. The parameter k is not exactly constant, it is dependent on temperature, but this behaviour is negligible. Figure 8 shows relatively short effective time delay $Tu < 1$ s and the rise time Tn about 13 s. This inclines, that first-order differential model is sufficient.

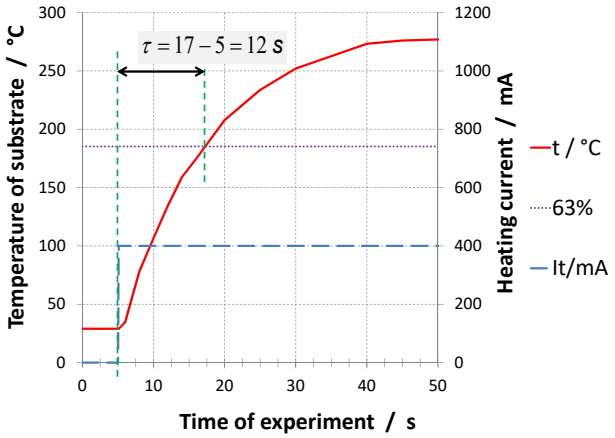

Figure 8. Step response of KBI2 as controlled system with highlighted time constant.
$t/$°C is time dependency of temperature
$It/$ mA is time dependency of heating current
63 % (dotted line) shows 63 % of steady-state, it helps to determine the time constant.

5. Conclusion

During our experiments, the KBI2 platform properties were discovered. Our department is forced to start using these platforms, because currently used platform are not made anymore, neither does their original manufacturer. Main purpose of this work was obtaining data needed for regulation utility design, eg. electronic circuits for temperature evaluation, regulator and a power element, which will control the heating power.

Acquired data shows, that temperature gradient cannot be avoided. In the area of interdigital electrodes approximately it may reach up to 30 °C. Experimental data allowed us to construct relatively simple and still sufficiently accurate formula for determination of temperature (2). Dynamic properties shows, that this system can be approximated as first order system well, time constant $\tau = 12$ s. This should not be a problem for regulation. Static characteristics are not included, but they shows, that the maximum heating current the element must handle is 500 mA with voltage around 8 V.

First experiment to be realized is classical regulation circuit as shown on Figure 9. Temperature sensor value is processed by Wheatstone bridge and differential amplifier. Operating temperature range 0-350 °C shall be mapped to unified voltage 0 - 5 V and subsequently evaluated by classical PI or PS regulator. Both classical PI operating amplifier based controller and software implemented PS regulator. The controller output will be amplified in a heating block consisting of a power transistor and operating amplifiers. [7] This heating block need to include a current limitation for protection of the platform in case of inappropriate tuning or controller malfunction.

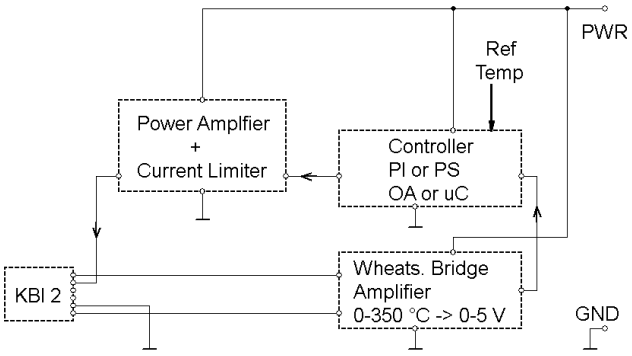

Figure 9. Block diagram of planned KBI 2 temperature regulation circuit.

Realization of the control circuit is currently being executed as part of solving a diploma thesis task.

Acknowledgments

This work was supported by Grant Agency of the Czech Republic (GACR), Project No. 17-13427S and also by NATO's Public Diplomacy Division in the framework of "Science for Peace" programme, project No.984597

References

[1] W. Göpel, K. D. Schierbaum, "SnO2 sensors:current status and future prospects", *Sensors and Actuators B* vol. 26-27 (1995) 1-12

[2] Tlesla Blatná a.s. *Kombinovaná senzorová platforma KBI2*, [Online]. Available:: http://www.tesla-blatna.cz/_soubory/katalogovy_list_kbi2.pdf downloaded February 2017

[3] Tlesla Blatná a.s. *Teplotní senzor Pt 1K* , [Online]. Available: http://www.tesla-blatna.cz/_soubory/katalogovy_list_pt1k.pdf downloaded February 2017

[4] FLIR T400. *Manual FLIR T-series.* Publ. No. 1558795. June 2008

[5] FLIR QuickReport. *Manual FLIR QuickReport*, v.1.2, Publ. 1558625, September 2008

[6] Isothermal Technology Limited *Manual GEMINI-R 550 Model 976*, Southport, England, Ed. December 2006

[7] J. Punčochář *Operační zesilovače v elektronice*, BEN technická literatura Praha, 1999